Pulse-Compression based Iterative Time-of-Flight Extraction of Dispersed Ultrasonic Guided Waves

Mehmet K. Yücel[1], Sina Fateri[1,2], Mathew Legg[1], Adam Wilkinson[2], Vassilios Kappatos[1], Cem Selcuk[1], Tat-Hean Gan[1]
Brunel University[1], Uxbridge, Middlesex, UB8 3PH, United Kingdom, Email: bic@brunel.ac.uk
Plant Integrity Ltd.[2], Granta Park, Great Abington, Cambridge, United Kingdom

***Abstract*—Ultrasonic Guided Wave (UGW) based Non-Destructive Testing (NDT) systems are widely used in numerous branches of industry, where the structural integrity of components carries vital importance. In those systems, signal interpretations might become challenging due to multi-modal and dispersive response of the structure under examination. This results in degradation of the signals in terms of Signal-to-Noise Ratio (SNR) and spatial/temporal resolution. This paper uses Maximal Length Sequences (MLS) to develop a novel signal processing technique by employing the Short-Time Fourier Transform (STFT), dispersion compensation and cross-correlation. The technique is applied to experimental multi-modal signals from an aluminum rod for performance verification. It is quantitatively validated that the technique noticeably improves the SNR of the guided wave response, and is able to derive an accurate time of flight of the individual wave modes and thus the propagation distance.**

***Index Terms*—Ultrasonic Guided Waves (UGW), Dispersion Compensation, Maximal Length Sequences (MLS), Cross-Correlation, Pulse Compression**

I. Introduction

Components used in numerous branches of industry are subject to various operational/environmental factors, which eventually damage the structural integrity of the components and cause health hazards and monetary losses. UGW testing is one of the several NDT techniques which has emerged in the last few decades as a reliable inspection tool for the swift assessment of the health of structures with varied geometries; principally for detection of flaws and corrosion. The theory of UGW is well-established and its characteristics can be represented with analytical solutions for structures such as pipes, plates and rods [1], [2]. In accordance with its well-established theory, it has been used for the inspection of a wide range of structures such as pipes, rods, cables and rails [3].

The emergence of advanced signal processing techniques and hardware development has led to enhanced defect detection, paving the way for a more confident classification of localization and severity of the structural discontinuity. Although such advances led to promising inspection tools, several challenges still exist. As UGW propagate through a medium, they experience attenuation depending on the material properties and the size of the medium. As a result of the attenuation, inspection range performance becomes severely limited and sensitive to noise generated by arbitrary sources. Moreover, depending on the material properties and the frequency spectrum of the propagating wave, UGW propagate in multiple wave modes, most of which can undergo severe dispersion in certain frequencies. The dispersive nature of the waves, which is a result of the dependence of the wave velocity on frequency, leads to broadening of the pulse. This temporal broadening leads to low spatial resolution, which means inaccurate localization of defects in NDT context. Therefore, signal interpretation needed for accurate localization and classification of the defects becomes more difficult. In order to address aforementioned problems, certain signal processing techniques have been proposed.

The Pulse Compression (PuC) technique, where autocorrelation properties of certain coded waveforms are exploited, has found use in many applications such as medical ultrasound [4] and material characterization [5]. PuC technique has been widely used in air-coupled ultrasonic testing where acoustic impedance mismatch-induced SNR degradation severely limits the inspection quality. Gan et al. used capacitive transducers to generate chirp signals in air-coupled imaging of solid samples [6] and wood samples [7]; Rodriguez et al. used air-coupled piezoelectric arrays to utilize Golay codes to inspect copper plates [8] and Ricci et al. used chirp signals to inspect forged steels with high attenuation [9]. Several studies have combined PuC with other techniques to further improve the SNR; Ricci et al. used chirp-based PuC combined with ℓ^1-norm total variation deconvolution [10] and Zhou et al. used wavelet transform to filter the noise and utilized Barker codes to perform PuC [11]. Nevertheless, further improvements are still required in dispersive regions of the frequency spectrum since temporal broadening of the pulse still exists and limits the performance of PuC.

Dispersion compensation techniques, where received time traces are compensated for the effects of dispersion, have been efficient for compressing wave packets and improving signal quality. Sicard et al. and Wilcox presented a method to compensate for the effect of dispersion from UGW signals in [12], [13]. Yamasaki et al. compared experimental and simulated time-reversed square pulses for dispersion compensation [14]. They qualitatively showed that the technique can improve the SNR. However, no attempts have been made to extract Time of Flight (ToF) and propagation distance in multi-modal response. Toiyama & Hayashi utilized PuC with dispersion compensation to enhance the SNR using chirp waveforms [15].

978-1-4799-6649-3/15/$31.00

However, the technique was only applied to single wave mode response and also no quantitative SNR improvement was presented. Marchi et al. combined PuC with Warped Frequency Transform (WFT) based dispersion compensation techniques in order to enhance the localization of the response of a steel cylindrical mass in an aluminum square plate [16]. However, the technique requires wavelength filtering to suppress the effect of multi-modal propagation. Zeng and Lin proposed a chirp-based dispersion pre-compensation technique using a *priori* knowledge of propagation distance [17]. However, the application of the technique is restricted with manual intervention rather than an automatic computerized analysis. Xu et al. proposed a wideband dispersion reversal technique to self-compensate fundamental wave modes in a steel plate [18]. However, in order to implement the WDR technique the propagation distance should be known. In one of the latest studies, Marchi et al. extended WFT based dispersion compensation to irregular wave guides [19], and then combined it with pulse compression to localize defects [20]. However, only triangular pulse excitation is used and no experimental validation is presented.

This paper makes use of Maximum Length Sequence (MLS) signals to present an automated technique using dispersion compensation and cross-correlation. Among various Time-Frequency representations (TFR) such as Wigner-Ville [21] and Scalogram [22], STFT is used to obtain spectrograms for visualization. The performance of the technique using MLS is assessed rigourously. It is shown that such a combination with cross-correlation can deliver SNR improvement and accurate extraction of ToF, and hence the propagation distance, in a multi-modal response.

The theoretical background is given in Section II and the proposed technique is described in Section III. The technique is applied to MLS waveforms in Section IV. The performance of the technique is also quantitatively compared in this section.

II. Theoretical Background

A. Dispersion Compensation

Dispersive wave modes spread out over time and space during propagation. Therefore, the spatial resolution of the waves can experience degradation. This makes the signal interpretations challenging [23]. Dispersion compensation techniques [12], [13] have been used to un-disperse the dispersed signals in order to achieve better spatial resolution. The algorithm makes use of a *priori* knowledge of the dispersion curve of a UGW mode and performs signal processing algorithm to map signals from the time domain to the spatial domain and reverse the dispersion process.

It is assumed that the transducer is ideal and only excites the guided wave modes of interest at the given location. The received time trace $\tilde{x}(t)$ at a given propagation distance, d may be modelled as given in [13],

$$\tilde{x}(t) = \sum_j \int_{-\infty}^{+\infty} A_j(\omega)\ F(\omega)\ e^{i\ (-k(\omega)\ d+\omega\ t)}\ d\omega \quad (1)$$

where, $A_j(\omega)$ is the reflection coefficient of each reflector, $F(\omega)$ is the Fourier transform of the input signal $f(t)$ excited at $d = 0$, ω is the angular velocity and $k(\omega)$ is the angular wavenumber defined as,

$$k(\omega) = \frac{\omega}{V_{ph}} \quad (2)$$

where V_{ph} is the phase velocity of the wave. The effect of dispersion can be corrected by choosing a centre frequency for dispersion compensation, f_c, and then shifting the other frequency components in order to centralize all frequency components at time $\tau = d/V_{gr}(f_c)$, where V_{gr} is the group velocity of the wave. Waveform $h(t)$, which is dispersion compensated for distance d, can then be written as,

$$h(t) = \sum_j \int_{-\infty}^{+\infty} A_j(\omega)\ G(\omega)\ e^{i\ (k(\omega)\ d+\omega\ (t-\tau))}\ d\omega \quad (3)$$

where $G(\omega)$ is the Fourier transform of the received signal $\tilde{x}(t)$ and $A_j(\omega)$ is the reflection coefficient of the reflectors (assumed frequency-independent and constant throughout this study). Once the compensated signal is acquired, this could be mapped back to the distance domain by converting time trace to distance trace using $V_{gr}(f_c)$. This approach, however, requires correct compensation for accurate projection on distance domain and correct information about $V_{gr}(f_c)$.

B. Pulse Compression

PuC technique is adopted to UGW from radar systems, where it is used to address the trade-off between detection of close reflectors, coverage range and hardware output power, and also to acquire the impulse response of a system. More information on PuC can be found in [24]. For the proper exploitation of the technique, a signal with a good autocorrelation function $ccf(x(t), x(t)) \cong \delta(t)$ is required [7]. Signals satisfying the desired autocorrelation condition that have been commonly used are linear/non-linear chirped sinusoids or pseudorandom binary sequences. Barker codes, MLS, Gold codes, Golay codes, Chaos sequence and Legendre sequence are examples of pseudorandom binary sequences used in the literature [25]. Following section contains brief information about MLS waveforms.

C. Maximal Length Sequences

MLS are generated using Linear Feedback Shift Registers (LFSR) with N-delay taps, resulting in a sequence of length $L = 2^N - 1$. The autocorrelation function of a N-length m-sequence, an important feature exploited in this study, is given as,

$$ccf_{a,a}(t) = \begin{cases} 1, & \text{lag} = 0 \\ 1/N & \text{lag} \neq 0. \end{cases} \quad (4)$$

Its has a δ-function like autocorrelation function and also has a flat spectral density with a near-zero DC component [26]. More information about m-sequences can be found in [27]. In this paper, MLS sequences are created using the work described in [28].

III. Proposed Technique

As mentioned in the previous section, UGW might experience dispersion as they propagate through a medium. A dispersed signal, as shown in Equation (1), could be compensated for dispersion via Equation (3) which compensates for frequency-dependent velocities of the existing wave modes. A dispersion compensated time trace would have good SNR and good defect localization. However, in multi-modal scenarios where modes are superposed, the interpretation of received signals could be difficult. In such cases, PuC technique can be used to increase the ability to accurately locate defects as well as improve the SNR.

A received UGW, after it has been dispersion compensated for correct propagation distance, denoted by $\tilde{x}(t)$, would ideally have good cross-correlation with $x(t)$; the signal excited by the transducer. Maximum value of cross correlation, $max(ccf(\tilde{x}(t), x(t)))$, would provide accurate localization of the reflection echo, thus the structural discontinuity in the context of ultrasonic NDT. An overall block diagram of the proposed technique is shown in Fig. 1.

The technique proposed in this study combines the dispersion compensation technique described in Equation (3) with the PuC technique in a brute-search manner to obtain $h_{d(1)}(t), \ldots, h_{d(n)}(t)$ the dispersion compensated values. The dispersed (received raw) signal $\tilde{x}(t)$ is iteratively compensated for dispersion (for a single wave mode) for a range of propagation distances $d(1), \ldots, d(n)$ and cross-correlated with the excitation signal. In every iteration, the maximum value of cross correlation $c_{d(1)}, \ldots, cd(n)$ between the dispersion compensated signal and the excitation signal are stored with its respective propagation distance value. Once the iterative search is completed, stored $max(ccf)$ values can be analyzed for various distances. After the maximum value of the stored $max(ccf)$ values is extracted, the corresponding distance value of this maximum will provide the propagation distance $d(i)$. Such analysis would also remove the need for a *priori* knowledge on the propagation distance for accurate dispersion compensation.

IV. Experimentation

A. Experimental Setup

Experimental verification of the proposed technique is performed on an aluminum cylindrical rod of 8-mm diameter. Group velocity dispersion curves for each wave mode propagating through the structure are acquired using Disperse [29] and shown in Fig. 2. The length of the structure was 2.15 meters and a shear-mode Lead Zirconium Titanate (PZT) transducer was attached to one end of the rod with a clamp. The clamping configuration was adjusted so that the force was applied uniformly to the transducer. The structure was interrogated in pulse-echo configuration (one transducer acting as both transmitter and receiver). A Teletest Unit [30] was used to drive the transducer. Power gain levels were fixed to 10 dB. The analog input sampling rate was set to 1 MHz. The received signals were not averaged deliberately in order to consider

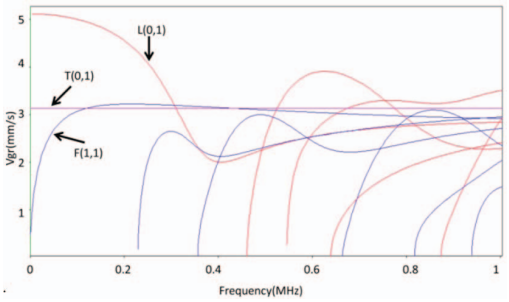

Fig. 2. Group velocity (V_{gr}) dispersion curves of an aluminum rod of 8mm diameter. The fundamental modes are shown by arrows; higher order flexural and longitudinal modes are shown in blue and red, respectively.

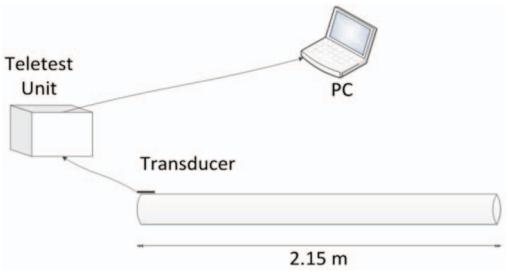

Fig. 3. Representative diagram for the experimental setup.

a challenging scenario in terms of the measurement noise. The received signals were transferred to a PC for analysis in MATLAB. A representative diagram of the experimental setup is illustrated in Fig. 3.

In this section, the received signals and the excitation signals, prior to being fed to the proposed algorithm, were normalized via ℓ^2-normalization. This normalization is performed to map both signals into a comparable level in terms of power in case transducer output had fluctuations.

The excitation signals were chosen as 65-sample MLS sampled at 250 kHz. The duration of the MLS excitation signals were thus 0.25 ms.

It must be noted that the excitation signals will be affected by the transfer function of the hardware and the transducer, which might deteriorate the cross correlation and dispersion compensation results [25]. An analysis of electrical and mechanical resonance of the type of transducer used in this paper can be found in [31] , which indicate these types of transducers have a sufficiently flat frequency response in the frequency range of concern.

B. Experimental Results

Signals fed from the hardware to the transducers are recorded to check the autocorrelation properties. The signal autocorrelation had a comparatively δ-function like shape, see Figure 4. Depending on the length of the rod and duration of the received signal, there can be multiple echoes and also multiple wave modes. In order to make it easier to demonstrate the technique, the received signals are windowed to acquire a certain window of time which corresponds to only two echoes.

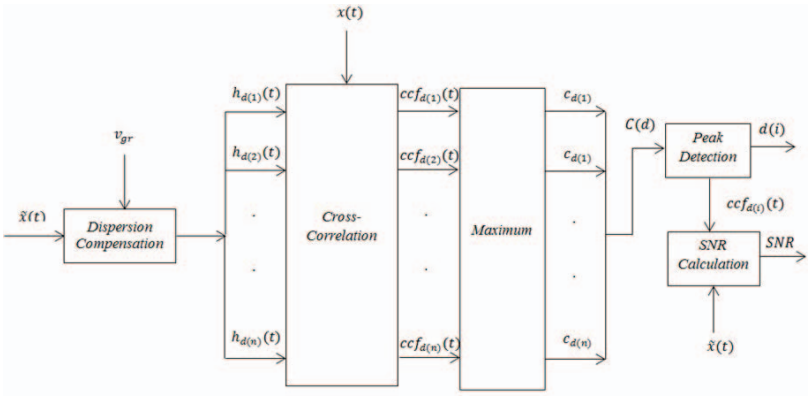

Fig. 1. Block diagram of the proposed technique.

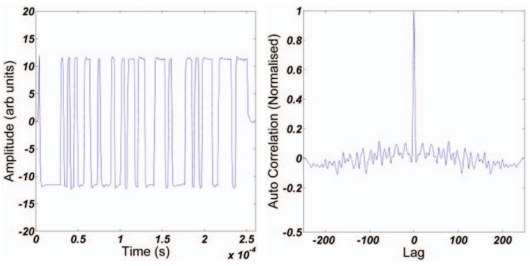

(a) (b)

Fig. 4. Plot of the MLS signal fed to the transducer in (a) time domain and (b) its auto correlation.

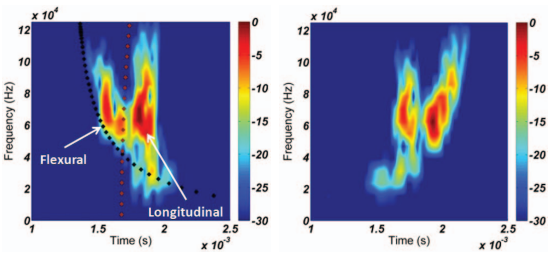

(a) (b)

Fig. 5. Measured signals' spectrograms with fundamental flexural (black dotted lines) and longitudinal (brown dotted lines) V_{gr} dispersion curve overlaid. Shown plots are (a) MLS and (b) dispersion compensated MLS. Two wave modes shown in (a) are the first echo of the fundamental flexural mode and the second echo of the fundamental longitudinal mode. Dispersion compensation is based on the flexural wave mode and it is performed for a travelled path of 4.3 m. Centre frequency for dispersion compensation is 48 kHz.

Spectrograms of the received signal is shown in Fig. 5(a). The overlaid dispersion curves verify that the windowed signals consist of the second echo of the fundamental longitudinal mode and the first echo of the fundamental flexural mode. It can be seen that the modes are superposed especially in the low frequency region. Due to the coupling of the transducer, the fundamental torsional wave mode is not excited. The center frequency for dispersion compensation is selected as 48 kHz. In order to achieve accurate cross correlation results, only the low frequency region of the received signals (<125 kHz, in line with excitation signal spectrums) are compensated. High frequency components of the signals, which were approximately 20 dB lower than the lower frequency regions, are ignored.

C. Flexural Mode Compensation

Fig. 6(a-b-c) show dispersed (ℓ^2-normalized), compensated (for flexural wave mode and for 4.3 m distance) and compressed MLS signals, respectively. The MLS signal, after compensation, shows two distinct and compressed peaks which account for the flexural and longitudinal modes, respectively. Following the dispersion compensation and cross correlation, as shown in Fig. 6(c), signal visibly has a better SNR value based on the flexural wave mode. Moreover, localization of structural discontinuities is also improved, as can be seen by the sharp peak in the compressed signal plots.

Quantification of the SNR improvement for experimental signals can be seen in Table I. SNR values were calculated as follows,

$$SNR = 20\ log_{10}\left(\frac{|P_e|}{\sigma_{x(t)}}\right), \tag{5}$$

where P_e is the echo's peak amplitude and σ is the standard deviation of $x(t)$ the signal under consideration [32]. The SNR improvement for MLS is found as 4.8 dB, which corresponds to a percentage SNR improvement of 26%.

The iterative search for the cross correlation maximum is performed for ranges between 0 and 10 meters with a step size of 0.01 m. Due to the multi-modal nature of the signal (the longitudinal mode has high cross correlation with excitation signal since it has low dispersion) as well as the influence of the transducer and the hardware, cross-correlation values are high in short distances, as shown in Fig. 8. These high cross correlation values at short distances can be tackled by looking at the maximum cross correlation of the wave mode of interest (not the entire signal). However, that would require accurate spatial/temporal separation of two modes and that might not be possible when modes are superposed. Due to the above mentioned high cross correlation values in short distances, the

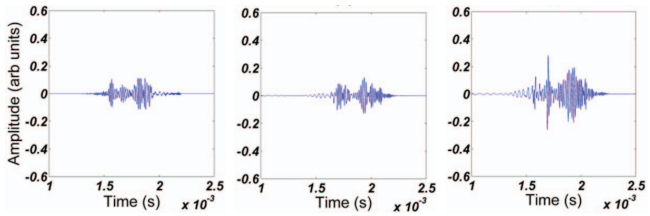

(a) (b) (c)

Fig. 6. Plots show time domain representations of (a) measured MLS signal, (b) dispersion compensated MLS signal, where the compensation has been performed for the flexural wave mode echo which has propagated a distance of 4.3 m, and (c) cross-correlation between excitation and dispersion compensated MLS signal.

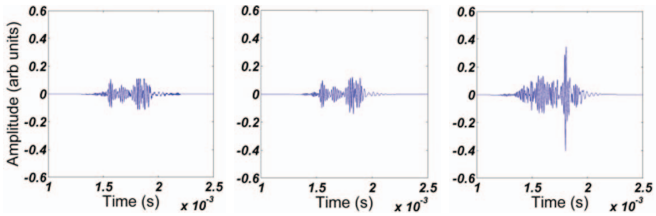

(a) (b) (c)

Fig. 7. Plots show time domain representations of (a) measured MLS signal, (b) dispersion compensated MLS signal, where the compensation has been performed for the longitudinal wave mode echo which has propagated as distance of 8.6 m, and (c) cross-correlation between excitation and dispersion compensated MLS signal.

maximum of cross correlation traces (shown in Fig. 8) after a certain distance is taken into account and the maximum of the rest is taken. Based on the empirical findings, this distance threshold value is chosen as 1 meter since after 1 m, cross correlation maximums actually go below the peak observed at the correct propagation distance. Once the results of the first meter are discarded, an accurate result is obtained; 4.29 meter, which yields 0.01 m error for propagation distance. It must also be noted that results are within 0.01 m confidence level due to step size of distance (0.01 m).

D. Longitudinal Mode Compensation

In order to achieve a complete analysis, the iterative technique has been implemented on the signals based on longitudinal wave mode compensation. All the parameters and signals used for the technique are the same as for the previous section, except for the dispersion compensation of the longitudinal wave mode. The results are shown in in Fig. 7. Unlike the flexural-based compensation, the dispersed raw signal (Fig. 7 (a), along with Fig. 6 (a), are approximately the same with the dispersion compensated signal (compensated for 8.6 m, which is the propagation distance for longitudinal mode's second echo) illustrated in Fig. 7(b). This similarity is due to the non-dispersive nature of the longitudinal wave mode. Once the compensated signals are compressed using cross correlation, MLS signal shows distinct, sharp peaks for the second wave packet which is the longitudinal wave mode. Quantification of the SNR improvement for longitudinal-based compensation of signal is given in Table I.

Results indicate 5.5 dB SNR improvement in this case. It must be noted that, since longitudinal is not dispersive, the initial peaks values are already high, as can be seen in Fig. 8(b). The percentage SNR improvement of MLS is reported as 24%, and it is negligibly lower than the flexural based compensation cases.

In addition to the SNR improvement factor, the extraction of the propagation distance is also analyzed using the iterative method for longitudinal based compensation and the results are shown in Fig. 8. Compared to the flexural based compensation, the iterative method fails for the longitudinal based compensation in terms of extracting an accurate propagation distance. The peak values of the traces shown in Fig. 8 are

TABLE I
TABLE SHOWS THE SNR VALUES FOR MLS EXCITATION SIGNALS. 'RAW' COLUMNS ARE THE SNR VALUES OF RAW SIGNALS, THE 'RESULT' COLUMNS ARE RESULTING SNRS OF DISPERSION COMPENSATED AND THEN COMPRESSED PULSES.

Signal	Mode	Raw [dB]	Result [dB]	Increase [%]
MLS	Longitudinal	22.5	28.0	24.7%
	Flexural	18.6	23.4	26.1%

different from the expected value (8.6 m). Another point of interest is that there is minimal variation in the maximum cross-correlation peak with distance for the longitudinal mode. This is an expected phenomenon because the longitudinal mode experiences minimal dispersion and hence the iterative technique would yield similar results in terms of the cross correlation maximums for several distances. Even though, in an ideal situation, the peak value of the longitudinal-based compensation trace should give the correct propagation distance, the sensitivity to the noise as well as the frequency response of the medium indicate the iterative technique can not extract the correct propagation distance based on longitudinal mode compensation.

E. Remarks and Recommendations

The frequency response of the transducer and the hardware is an influential factor for the proposed iterative technique. Although accurate propagation distance results are obtained, due to measurement noise transducer/hardware effect (even assumed in negligible levels) and the response of the structure, the frequency contents of the received signal were not the same as the excited signal. As a result, the extracted propagation distances had minor errors (Fig. 8).

The technique was also implemented with a lower distance increment (0.0001 m). It was observed that the technique had the same peak values at close distances, which means multiple maximum propagation distances were extracted. It can be argued that this depends on the resolution of the V_{gr} dispersion curve data used to compensate the signals for dispersion. In this paper, the V_{gr} dispersion curve data was interpolated to cover a wide frequency range. This interpolation, however, could produce minor errors in certain frequencies' V_{gr} values. These minor errors might not be visible up to certain distance

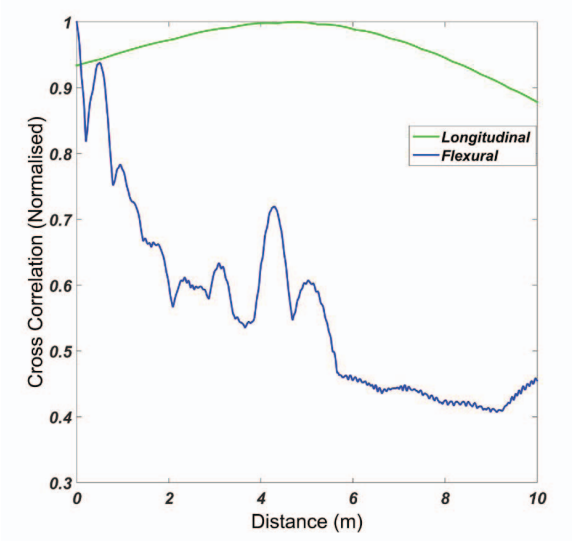

Fig. 8. Plot shows the results of the iterative technique; maximum cross-correlation trace, as a function of distance, of MLS (blue) signal (compensation performed on flexural). Longitudinal based compensation result are shown in green lines. The iterative technique failed to extract the correct propagation distance (8.6 m for longitudinal) in the case of longitudinal compensation. Results are obtained by applying the iterative technique with 0.01 m distance resolution.

increment, yet it was visible in (0.1 mm) distance increment resolution. The relatively insufficient resolution of V_{gr} data could also be presented as the reason of unsuccessful propagation distance extraction for the longitudinal mode presented in Section IV, as this wave mode is dispersed in a minor way that V_{gr} data might not resolve.

V. Conclusions and Future Work

In this paper a novel iterative technique comprising dispersion compensation, STFT and cross-correlation was presented using broadband MLS excitation. The technique iteratively searches for the correct propagation distance using a *priori* knowledge of the group velocity dispersion curve. The accurate propagation distance of individual wave modes were successfully extracted via compressing the dispersion compensated signals using cross-correlation.

The results given by MLS excitation were quantitatively assessed. Despite the existence of the measurement noise and superposed wave modes, the iterative search technique extracted an accurate propagation distance for MLS with 1 cm error over a propagation distance of 4.3 meters. Moreover, considerable SNR improvement (Table I) was achieved. The technique was compared for different wave modes (dispersive flexural and non-dispersive longitudinal) in terms of the propagation distance extraction and the SNR improvement results. It was observed that similar SNR improvement can be achieved for both dispersive and non-dispersive wave modes, though the propagation distance extraction works more accurately for dispersive wave modes. Results show that the proposed technique and MLS waveforms are promising for the automated inspection of cylindrical structures.

Future work will include a thorough noise analysis for performance assessment of the technique using MLS, comparison with other coded waveforms used frequently in UGW applications and a thorough signal modelling to establish a framework for the proposed technique.

VI. Acknowledgement

The authors would like to thank Dr. M. Livadas and Dr. N. V. Boulgouris for their comments and guidance.

References

[1] H. Lamb, "On waves in an elastic plate," *Proceedings of the Royal Society of London Series A, Containing papers of a mathematical and physical character*, pp. 114–128, 1917.

[2] K. F. Graff, *Wave motion in elastic solids*. Courier Dover Publications, 1975.

[3] J. Rose, "Successes and challenges in ultrasonic guided waves for NDT and SHM," in *National Seminar&Exhibition on Non-Destructive Evaluation*, Tiruchirappalli, India, 2009.

[4] T. Misaridis and J. A. Jensen, "Use of modulated excitation signals in medical ultrasound. part 1: Basic concepts and expected benefits," vol. 52, no. 2, pp. 177–191, 2005.

[5] R. E. Challis and V. Ivchenko, "Sub-threshold sampling in a correlation-based ultrasonic spectrometer," *Measurement Science and Technology*, vol. 22, no. 2, 2011.

[6] T. H. Gan, D. A. Hutchins, D. R. Billson, and D. W. Schindel, "The use of broadband acoustic transducers and pulse-compression techniques for air-coupled ultrasonic imaging," *Ultrasonics*, pp. 181–194, 2011.

[7] T. H. Gan, D. Hutchins, and R. Green, "Noncontact, high-resolution ultrasonic imaging of wood samples using coded chirp waveforms," *IEEE Trans. on Ultrasonics, Ferroelectrics and Frequency Control*, vol. 52, no. 2, pp. 280–288, 2005.

[8] M. Garcia-Rodriguez, Y. Yañez, M. J. Garcia-Hernandez, J. Salazar, A. Turo, and J. A. Chavez, "Application of Golay codes to improve the dynamic range in ultrasonic Lamb waves air-coupled systems," *NDT & E International*, vol. 43, no. 8, pp. 677–686, 2010.

[9] M. Ricci, L. Senni, P. Burrascano, R. Borgna, S. Neri, and M. Calderini, "Pulse-compression technique for the inspection of forged steel with high attenuation," *Insight-Non Destructive Testing and Condition Monitoring*, vol. 52, no. 2, pp. 91–95, 2012.

[10] M. Ricci, S. Callegari, S. Caporale, M. Monticelli, L. Battaglini, M. Eroli, L. Senni, R. Rovatti, G. Setti, and P. Burrascano, "Exploiting non-linear chirp and sparse deconvolution to enhance the performance of pulse-compression ultrasonic NDT," in *IEEE International Ultrasonics Symposium (IUS)*, 2012.

[11] Z. Zhou, B. Ma, J. Jiang, G. Yu, K. Liu, D. Zhang, and W. Liu, "Application of wavelet filtering and Barker-coded pulse compression hybrid method to air-coupled ultrasonic testing," *Nondestructive Testing and Evaluation*, vol. 29, no. 4, pp. 297–314, 2014.

[12] R. Sicard, J. Goyette, and D. Zellouf, "A numerical dispersion compensation technique for time recompression of Lamb wave signals," *Ultrasonics*, vol. 40, no. 1, pp. 727–732, 2002.

[13] P. Wilcox, "A rapid signal processing technique to remove the effect of dispersion from guided wave signals," *IEEE trans. on Ultrasonics, Ferroelectrics and Frequency Control*, vol. 50, no. 4, pp. 419–427, 2003.

[14] T. Yamasaki, S. Tamai, and M. Hirao, "Optimum excitation signal for long-range inspection of steel wires by longitudinal waves," *NDT&E International*, vol. 34, no. 3, pp. 207–212, 2001.

[15] K. Toiyama and T. Hayashi, "Pulse compression technique considering velocity dispersion of guided wave," in *Review of Progress in Quantitative Nondestructive Evaluation: 34th Annual Review of Progress in Quantitative Nondestructive Evaluation*, vol. 975, no. 1. AIP Publishing, 2008, pp. 587–593.

[16] L. De Marchi, A. Perelli, and A. Marzani, "A signal processing approach to exploit chirp excitation in Lamb wave defect detection and localization procedures," *Mechanical Systems and Signal Processing*, vol. 39, no. 1, pp. 20–31, 2013.

[17] J. Lin and L. Zeng, "Chirp-based pre-compensation for high resolution Lamb wave inspection," *NDT &E International*, vol. 61, pp. 35–44, 2013.

[18] K. Xu, D. Ta, B. Hu, P. Laugier, and W. Wang, "Wideband dispersion reversal of Lamb waves," *Ultrasonics, Ferroelectrics and Frequency Control, IEEE Transactions on*, vol. 61, no. 6, pp. 997–1005, 2014.
[19] L. De Marchi, A. Marzani, and M. Miniaci, "A dispersion compensation procedure to extend pulse-echo defects location to irregular waveguides," *NDT & E International*, vol. 54, pp. 115–122, 2013.
[20] L. De Marchi, A. Marzani, M. Miniaci, A. Perelli, and N. Testoni, "Localization of defects in irregular waveguides by dispersion compensation and pulse compression," in *SPIE Smart Structures and Materials+ Nondestructive Evaluation and Health Monitoring*. International Society for Optics and Photonics, 2013, pp. 869 517–869 517.
[21] W. Prosser, M. D. Seale, and B. T. Smith, "Time-frequency analysis of the dispersion of lamb modes," *The Journal of the Acoustical Society of America*, vol. 105, no. 5, pp. 2669–2676, 1999.
[22] Z. Peng, F. Chu, and Y. He, "Vibration signal analysis and feature extraction based on reassigned wavelet scalogram," *Journal of Sound and Vibration*, vol. 253, no. 5, pp. 1087–1100, 2002.
[23] J. Krautkramer and H. Krautkramer, *Ultrasonic testing of materials*. Springer Verlag, 1990.
[24] M. I. Skolnik, "Introduction to radar," *Radar Handbook*, vol. 2, 1962.
[25] D. Hutchins, P. Burrascano, L. Davis, S. Laureti, and M. Ricci, "Coded waveforms for optimised air-coupled ultrasonic nondestructive evaluation," *Ultrasonics*, vol. 54, no. 7, pp. 1745–1759, 2014.
[26] S. W. Golomb, *Shift Register Sequences*. Laguna Hills, CA: Aegean Park Press, 1982.
[27] M. Ricci, L. Senni, and P. Burrascano, "Virtual instrument for air-coupled ultrasound NDT application based on psuedo-noise sequences." *relation*, vol. 1000, p. 1, 2011.
[28] T. Wiens, "Kasami sequences, m-sequences, linear feedback shift registers," http://www.mathworks.com/matlabcentral/fileexchange/22716-kasami-sequences--m-sequences--linear-feedback-shift-registers/content/coding_1_02/kasami.m, 2009. Last accessed Sep. 2014.
[29] B. Pavlakovic, M. J. S. Lowe, D. N. Alleyne, and P. Cawley, "Disperse:a general purpose program for creating dispersion curves," in *Review of Progress in Quantitative Nondestructive Evaluation*, D. O. Thompson and D. E. Chimenti, Eds. New York: Plenum, 1997, vol. 16, p. 185192.
[30] P. Mudge, "Field application of the Teletest long range ultrasonic testing technique," *Insight*, vol. 43, no. 2, 2001.
[31] B. Engineer, "The mechanical and resonant behaviour of a dry coupled thickness-shear PZT transducer used for guided wave testing in pipe line," Ph.D. dissertation, School of Engineering and Design, Brunel University, London, 2013.
[32] E. Pardo, J. L. San Emeterio, M. A. Rodriguez, and A. Ramos, "Noise reduction in ultrasonic NDT using undecimated wavelet transforms," *Ultrasonics*, vol. 44, pp. 1063–1067, 2006.